International Journal of Pharmaceutics 388 (2010) 223–230

Contents lists available at ScienceDirect

International Journal of Pharmaceutics

journal homepage: www.elsevier.com/locate/ijpharm

The in vitro and in vivo anti-tumor effect of layered double hydroxides nanoparticles as delivery for podophyllotoxin

Lili Qin[a,1], Meng Xue[a,1], Wenrui Wang[a], Rongrong Zhu[a], Shilong Wang[a,*], Jing Sun[b], Rui Zhang[c], Xiaoyu Sun[a]

[a] Shanghai Key Laboratory of Cell Signaling and Diseases, School of Life Science and Technology, Tongji University, Shanghai 200092, PR China
[b] First Maternity and Infant Health Hospital, PR China
[c] School of Chemical Engineering, Nanjing Forestry University, Nanjing, Jiangsu 210037, PR China

ARTICLE INFO

Article history:
Received 18 September 2009
Received in revised form
16 December 2009
Accepted 22 December 2009
Available online 5 January 2010

Keywords:
Nanoparticle
Drug delivery
Anti-tumor effect
In vitro test
In vivo test

ABSTRACT

In this research, we intercalated anti-tumor drug podophyllotoxin (PPT) into layered double hydroxides (LDHs) and investigated the in vitro cytotoxicity to tumor cells, the cellular uptake and in vivo anti-tumor inhibition of PPT-LDH. The nanohybrids were prepared by a two-step method with the size of 80–90 nm and the zeta potential of 20.3 mV. The in vitro cytotoxicity experiment indicated that PPT-LDH nanoparticles show better anti-tumor efficacy than PPT and are more readily taken up by Hela cells. PPT-LDH shows a long-term suppression effect on the tumor growth, and enhances the apoptotic process of tumor cells. The in vivo tests reveal that delivery of PPT via LDH nanoparticles is more efficient, but the mice toxicity of PPT in PPT-LDH hybrids is reduced in comparison with PPT alone. Pharmacokinetics study displays a prolonged circulation time and an increased bioavailability of PPT-LDH than PPT. These observations imply that LDH nanoparticles are the potential carrier of anti-tumor drugs in a range of new therapeutic applications.

1. Introduction

Podophyllotoxin (PPT), known as podofilox, is a non-alkaloid toxin in the lignan family. The main active antiwart component is podophyllin, an herbal extract of Podophyllum, and used as one of the main treatments for genital warts (Canel et al., 2000; Imbert, 1998). PPT and its derivatives inhibit the growth of epithelial cell infected by human papilloma virus (HPV) in epidermis (Longstaff and Von Krogh, 2001). Podophyllotoxin is the pharmacological precursor of the important anti-cancer drug etoposide against various cancers, such as small cell lung cancer (Arnold, 1979), testicular carcinoma (Greenspan et al., 1950), and lymphomas (Gordaliza et al., 2000). However, their poor water solubility, metabolic inactivation, drug resistance, myelosuppression and poor bioavailability have limited their success in direct applications (Van-maanen et al., 1998; Hainswoth et al., 1985; Shah et al., 1989). Therefore, an efficient drug delivery system is desired to overcome these drawbacks and improve the clinical therapy.

In recent years, many carriers have been developed, and can be general classified into four major groups: viral carriers, organic cationic compounds, recombinant proteins and inorganic nanoparticles (Azzam and Domb, 2004; Garnett, 2004). Inorganic nanoparticles have recently been receiving considerable attention. Layered double hydroxides (LDHs) are one of the inorganic nanoparticles. LDHs, also known as hydrotalcite-like compounds, are a family of anionic clay materials, exemplified by the natural mineral hydrotalcite $[Mg_6Al_2(OH)_{16}CO_3{\cdot}4H_2O]$. Most LDH minerals can be described with the general formula $[M_{1-x}^{2+}M_x^{3+}(OH)_2][A_{x/n}^{n-}]{\cdot}mH_2O$, where M^{2+} and M^{3+} represent di- and tri-valent cations octahedrally coordinated to hydroxyl ions, A^{n-} is the interlayer organic or inorganic anion, m is the number of interlayer water, and $x = M^{3+}/(M^{2+} + M^{3+})$ stands for the layer charge density of LDH (Seida and Nakano, 2002; Kwon and Choy, 2003). In recent years, LDH has been found to possess promising applications in biomedicine due to their unique anion exchange capability, controlled release and protection of the payload. Many LDH compounds intercalated with bioorganic anions such as DNA (Choy et al., 1999, 2001; Kwak et al., 2004; Hofer et al., 2004), amino acids (Aisawa et al., 2001; Zhang et al., 2004; Hibino and Nishiyama, 2004; Wong et al., 1999; Nakayama et al., 2002), anionic polymers (Wang et al., 2005), pesticides (Zhang et al., 2005, 2006), and drugs (Ambrogi et al., 1995; Li et al., 2004; Del Arco et al., 2000; Gutierrez et al., 1995; Qin et al., 2008) have been prepared successfully. Special interests have focused on exploring the possibilities of using LDH-drug delivery systems to deliver anti-inflammatory (Ambrogi

* Corresponding author. Tel.: +86 21 65982595; fax: +86 21 65982286.
E-mail address: wsl@tongji.edu.cn (S. Wang).
[1] These authors contributed equally to this work.

0378-5173/$ – see front matter © 2009 Elsevier B.V. All rights reserved.
doi:10.1016/j.ijpharm.2009.12.044

et al., 2006) or anti-cancer drugs (Tyner et al., 2004). Furthermore, this drug delivery system can be modified to specific cells or organs, thereby expanding its application range (Xu et al., 2006).

In the previous research, we had reported that PPT-LDH nanohybrids could be used as a reservoir of PPT molecules and the w/w loading is 34%. (Xue et al., 2007). The purpose of this study was to investigate in vitro and vivo anti-tumor efficiency of LDH as PPT delivery. We found that both in vitro and in vivo studies PPT-LDH nanohybrids showed better anti-tumor effect than PPT alone and it was also suggested that PPT-LDH had a significant tumor inhibition rate with 46.4% and reduced the toxicity effect to mice.

2. Materials and methods

2.1. Materials

Podophyllotoxin was a kind gift from University of Science and Technology of China. RPMI-1640, fetal calf serum (FCS), penicillin G, streptomycin, and trypsinase were obtained from GIBCO BRL (Grand Island, NY, USA). Dimethyl sulphoxide (DMSO), [3-(4, 5-dimethylthiazol-2-yl)-2 and 5-diphenyltetrazolium bromide] (MTT) were purchased from Sigma Chemical Co. (St. Louis, MO, USA). The water used for all applications was decarbonated by boiling.

Female nude mice weighing 18–22 g were purchased from Shanghai Laboratory Animal Co. (SLAC), Ltd. and hosted in stainless steel cages in a ventilated animal room. Room temperature was maintained at 24 ± 2 °C, and relative humidity at 50 ± 10%, in a 12 h light/dark cycle. Distilled water and sterilized food for mice were available ad libitum. All animals were treated following the protocol approved by the Institutional Animal Care and Use Committee at Shanghai Institute of Materia Medica, Chinese Academy of Sciences.

2.2. Preparation of PPT-LDH

The Mg–Al/LDH containing tyrosine (Tyr-LDH) was prepared by coprecipitation (variable pH method) under N_2 atmosphere to minimize the contamination by atmospheric CO_2 following the conventional route (Taylor, 1984). The mixed solution of 1 M $Mg(NO_3)_2{\cdot}6H_2O$ and $Al(NO_3)_3{\cdot}9H_2O$ (Mg:Al ratio of 3:1) was added drop-wise to an aqueous solution of 1 M tyrosine with vigorous stirring under a nitrogen atmosphere at room temperature. The final solution pH was adjusted to 10.0 ± 0.2 by drop-wise addition of 1 M NaOH solution, and stirred vigorously at 80 °C for 5 h under N_2 atmosphere with occasional adjustment of pH. The resulting precipitates were washed, and vacuum-dried for subsequent investigations.

PPT-LDH nanohybrids were prepared by an ion-exchange process. The freshly prepared Tyr-LDH suspension was added to a 0.1 M podophyllotoxin solution (pH previously adjusted to 12 with 1.0 M NaOH). The solid was kept in suspension under stirring and nitrogen atmosphere at 80 °C for 5 h. Resulting precipitates were filtered, washed thoroughly with decarbonated water, and dried overnight *in vacuo* at 60 °C.

2.3. Characterization

The average particle size (*z*-average size) and size distribution were measured using photon correlation spectroscopy (LS230 Beckman Coulter) at 25 °C under a fixed angle of 90° in disposable polystyrene cuvettes. The measurements were conducted using a He–Ne laser of 633 nm. Zeta potential of LDH nanoparticles was analyzed by Nano ZS, Malvern Instrument. Fourier transform infrared spectra (FTIR) were obtained on a Bruker Vector 22 spectrophotometer in the range of 4000–500 cm^{-1} using the standard KBr disk method (sample/KBr = 1/100). Transmission electron micrograph (TEM) samples were obtained using a JEOL 1230 Transmission Electron Microscope at an acceleration voltage of 200 kV.

2.4. In vitro anti-tumor effect of PPT-LDH

The anti-tumor effect of LDH, PPT and PPT-LDH against Hela cells was examined by cell viability test. Cell lines were routinely cultured in RPMI-1640 supplemented with 10% fetal bovine serum and incubated at 37 °C in a 5% CO_2 humid incubator. Typically, 100 μl of cells were plated at a density of approximate 2×10^4 cells per well in a 96-well plate, and were subsequently incubated at 37 °C in a 5% CO_2 humid incubator for 24 h. Then PPT, PPT-LDH and LDH were added to each group (triplicate wells) with the concentration of 20 μg/ml and the incubation was continued as indicated above for 24, 48 and 72 h, followed by adding 20 μl (5 mg/ml) of MTT dye solution was added to each well for 4 h at 37 °C. After removal of the MTT dye solution, cells were treated with 150 μl DMSO and the absorbance at 590 nm was quantified using a microplate reader (ELX 800 UV, BIO-TEK, USA). Cell viability was calculated with the following formula:

$$\text{Cell viability}\ (\%) = \frac{OD_{590(\text{sample})} - OD_{590(\text{blank})}}{OD_{590(\text{control})} - OD_{590(\text{blank})}} \times 100\%$$

2.5. Cellular uptake of PPT-LDH

The cellular uptake of PPT-LDH nanoparticles by Hela cells was examined with fluorescence and transmission electron micrograph (TEM) image. In a 96-well plate, Hela cells were seeded at a density of 2×10^4 cells per well and incubated for 24 h. FITC was dissolved in absolute ethanol and 100 μl FITC was mixed with 100 μl PPT-LDH respectively for 10 min in dark. Then the mixture was washed twice with cell medium. Cells were then incubated with PPT-LDH-FITC suspension for 12 h (finally the concentration was 20 μg/ml). Cells were washed twice with PBS (pH 7.4) and directly observed under a fluorescence microscope (Nikon Japan, ECLIPSE E6000).

Hela cells with 2×10^4 cells in each well and PPT-LDH at the final dose (20 μg/ml) were incubated in 96-well tissue culture plate in CO_2 incubator for 24 h. Hela cells treated with PBS (pH = 7.4) were taken as the control. For TEM analysis, Hela suspension was centrifuged at 1000 r min^{-1} for 10 min. The pellet was washed three times by PBS (pH = 7.4) and fixed with 2.0% glutaraldehyde in washing solution. After washing, the cells were post-fixed for 4 h with 1% osmium tetroxide in 0.1 M sodium cacodylate buffer, followed by being dehydrated in a series of ethanol solution (50, 70, 90, 95, 100 and 100%). Finally Hela cells were incubated in the mixture of LR white and ethanol (2:1) for 12 h and (1:1) for 2 h at 4 °C, and embedded in LR white for 72 h at 37 °C. Ultrathin sections (70 nm) were cut and transferred on 200-mesh grids, stained with uranyl acetate, counter-stained with lead citrate according to standard methods, observed with JEM-1230 TEM at 80 KV (JEOL Ltd., Japan) and taken pictures with GATAN 792 (Gatan Inc., USA).

2.6. Colony forming efficiency assay

Colony forming efficiency assay was performed to evaluate the effectiveness of the tested agents against long-term cancer cell proliferation. Hela cells were cultured, suspended in RPMI1640 with 10% pasteurized FCS, and seeded in a 24-well flat-bottomed plate filled with 200 cells/ml and stabilized by incubation for 24 h at 37 °C. Then, PPT.PPT-LDH and LDH were added at the concentration of 0, 0.001, 0.01, 0.1, 1 μg/ml and incubation at 37 °C. After the medium was replaced by the fresh medium, incubation was continued for a

total incubation period of 14 days. The medium was removed from the cells, which were successively washed with PBS and immobilized with MeOH. After removing MeOH, the cells were stained with Giemsa staining solution for 30 min, excess stain was washed with PBS solution and colonies (>50 cells) were counted using a light microscope. Plating efficiency of each treatment was calculated as the following formula:

$$\text{Colony form rate } \% = \frac{\text{number of viable colonies formed}}{\text{total number of cells plated}} \times 100\%$$

2.7. Fluorescence activated cell sorter (FACS) analysis

The number of the apoptosis cells was determined with the Annexin V-PI detection kit. Hela cells with 1×10^6 were cultured, suspended in RPMI1640 with 10% pasteurized FCS, and seeded in a 24-well flat-bottomed plate and incubated for 24 h at 37 °C. The PPT, PPT-LDH and culture medium only were added to each group with the concentration of 20 μg/ml and the incubation was continued for 48 h. Then the cells were harvested and washed with PBS, then PI and Annexin V added directly to the cell suspension in the binding buffer (10 mM HEPES, 140 mM NaCl, 2.5 mM $CaCl_2$, pH 7.4). The cells were incubated in the dark for 15 min at 37 °C and submitted to FACS analysis on a Beckton–Dickinson (Mountain View, CA) spectrophotometer.

2.8. In vivo anti-tumor effects of PPT-LDH nanoparticles

PPT-LDH and PPT administrated intravenously was determined in healthy female nude mice. Hela cells were collected from ascites, and were adjusted to a concentration of 1×10^7 cells/ml in normal saline. For tumor implantation, 0.2 ml of Hela cells suspension was injected subcutaneously into each mouse in the right flank. After tumor inoculation, mice were randomly sorted into treatment groups of 12 mice each and received a single daily intraperitoneal injection of saline (control), PPT in 20% ethanol (5 mg/kg) and PPT-LDH (equimolar to PPT in the ethanol formulation) for 3 weeks. Tumor volume and body weight were monitored daily. Tumor volume was calculated based on the equation $(a \times b^2)/2$, where "a" was the length and "b" was the width of the tumor. Mice were sacrificed 24 h after the last administration. Tumors were separated and weighed to determine the tumor inhibition rate, which is calculated according to the formula:

$$\text{Inhibition rate } \% = 1 - \frac{\text{tumor weight in test group}}{\text{tumor weight in control}} \times 100\%$$

2.9. Pharmacokinetics properties of PPT-LDH nanoparticles

PPT-LDH and PPT formulations were injected intraperitoneally at the PPT dose of 10 mg/kg body weight, and each group consisted of four to five mice. Blood samples were collected in heparin-containing tubes at the designated times (10, 20, 40 min and 1, 2, 4, 8, 16, 32, 48 and 60 h) via quickly removing the eyeball from the socket with a pair of tissue forceps. Plasma was isolated by centrifugation (10 min at 5000 r/min), stored at −20 °C. 1 ml of plasma was mixed with 0.4 ml of ethyl acetate. After vortex mixing for 10 min and centrifuging for 10 min (13,000 r/min), the organic phase was separated and evaporated, and the residue then reconstituted with 200 μl of mobile phase and was mixed in a vortex mixer for 10 min. Upon centrifugation at 13,000 r/min for 10 min, a portion (20 μl) of the reconstituted sample was injected on the chromatography column. PPT concentration was analyzed by HPLC using an Discovery C18 column (250 mm × 4.6 mm, 5 μm particle size) and an isocratic program with a solvent system of methanol/water 45:55 (v/v) with a UV detector at 290 nm (flow rate 1 ml/min).

Pharmacokinetic parameters, including area under the curve (*AUC*), total body clearance (*CL*) and plasma half-life for the distribution and elimination phase ($t_{1/2}\alpha$, $t_{1/2}\beta$) were assessed using a software program (3p87). The structural model was two compartment. All statistical analysis was performed using statistical package for social sciences (SPSS, version 11.0).

2.10. Statistical analysis

For statistical analysis, the data of cytotoxicity and colony forming efficiency was presented as the mean ± S.D. of three independent experiments. One-way ANOVA followed with *t*-test was performed using SPSS program, and levels of significance were represented in each result.

3. Results and discussion

3.1. Nanohybrid physical feature

The particle size distribution of PPT-LDH nanohybrids is narrow, with a nominal mean hydrodynamic diameter of 80–90 nm (Fig. 1A) and a zeta potential of 20.3 mV (Fig. 1B). Intercalation of PPT into LDH was also confirmed by the presence of characteristic PPT vibration in the FTIR spectrum (Fig. 2). For example, the absorption band at 1770 cm^{-1} is the stretching vibration of C=O associated with the backbone of the aromatic ring.

3.2. In vitro anti-tumor effect and cellular uptake of PPT-LDH

The anti-cancer efficiencies of PPT-LDH and PPT with 20 μg/ml were evaluated by bioassay using Hela cells. Fig. 3 shows the time-dependent cell viability. PPT and PPT-LDH suppressed the cell viability of tumor cells, whereas LDH itself had no significant effect. Moreover, PPT-LDH had higher tumor suppression efficiency compared to PPT at these incubation times. The result indicated that PPT-LDH had better effect in cancer treatment than PPT as demonstrated that the cell viability of PPT-LDH was much lower than that of PPT only after 3 days treatment. It seemed that PPT in the hybrid system could reach the tumor cell membrane without any early decomposition, since the PPT molecules were stabilized when they were entrapped in LDH. Meanwhile, PPT-LDH nanohybrids could

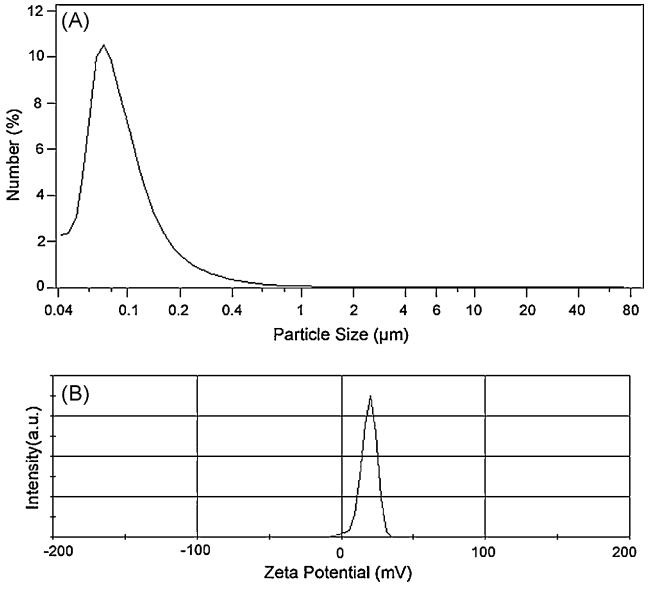

Fig. 1. (A) Particle size distribution and (B) zeta potential distribution of PPT-LDH nanoparticles.

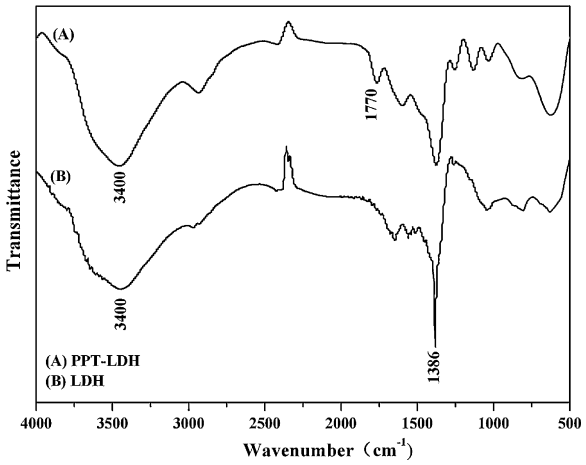

Fig. 2. Infrared spectra of (A) PPT-LDH and (B) LDH.

be more quickly taken up by Hela cells and the property of controlled released of PPT-LDH could also prolong the exposure time allowed for more tumor cells to be affected in order to increase the drug efficiency (Choy et al., 2004; Xu et al., 2008; Tyner et al., 2004; Yuan et al., 2008).

In order to detect the PPT-LDH nanoparticles internalized into the cells, the FITC combined with PPT-LDH was added to the cell culture medium. As shown in Fig. 4(A and B), PPT-LDH-FITC was internalized into the cells as the fluorescence cells were observed in the fluorescence microscope. It suggested that FITC binding with PPT-LDH were more easily taken up by Hell cells compared with FITC, which cannot be achieved by free FITC diffusion (Xu et al., 2008). Furthermore, PPT-LDH nanoparticles uptake had been evidenced by the cell TEM images. It showed ultrastructural alterations in Hela cells exposed 20 μg/ml PPT-LDH. Fig. 4(C) shows the typical ultrastructural appearance of healthy, untreated Hela cells characterized as a single large, elliptical shaped nucleus that contained a single, well defined nucleolus, as well as a granular cytoplasm sparsely filled with fewer organelles. As shown in Fig. 4(D and E), nucleoli were located near the periphery of nuclear membrane in PPT-LDH treated group. Nanoparticles were taken up by Hela cells. Single or aggregated nanoparticles were found in the cytoplasm of cells. Most of the mitochondria lost cristae translocated into the nucleus.

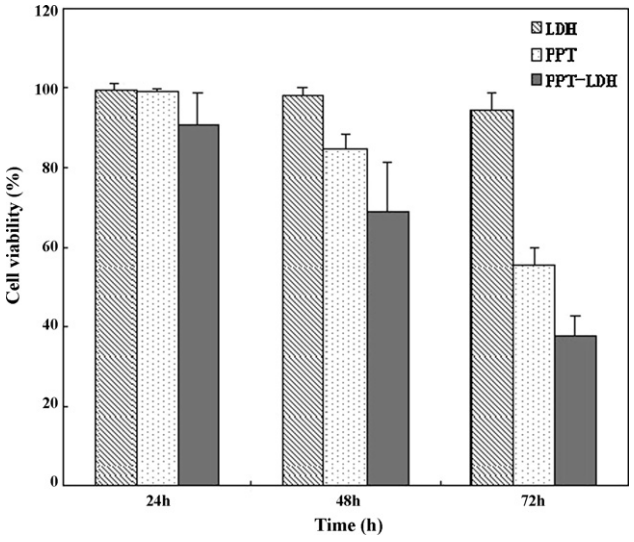

Fig. 3. Survival ratio of Hell cells treated with LDH, PPT and PPT-LDH with different times. Results represented means of three independent experiments.

Obviously, big bubbles were observed around the nanoparticles in the cytoplasm of cells. At higher magnification the aggregated PPT-LDH was seen to insert into Hela cells by cellular endocytosis in Fig. 4(F and G). Therefore, PPT-LDH nanoparticles crossed through the tumor cell membrane and then influence the cells.

3.3. Colony forming efficiency assay

The long-term suppression effect treated for 14 days with PPT, PPT-LDH and LDH was examined with the clonogenic assay. In this assay, an effective anti-tumor treatment results in a reduction in cell colony formation. As shown in Fig. 5, Hela cells colony forming decreased significantly when the concentrations of PPT and PPT-LDH increased. At a lower drug concentration 0.001, 0.01, 0.1 and 1 μg/ml, PPT-LDH treatment showed stronger anti-tumor effect than PPT alone. However, the LDH treated group did not show obvious suppression to the tumor growth, suggesting that the observed anti-tumor activity was not caused by the LDH but by PPT only. The results demonstrated that PPT-LDH had an excellent controlled released property (Xu et al., 2008; Tyner et al., 2004) and anti-cancer suppression effect in the long-term culture.

3.4. FACS analysis to detect apoptosis cells

Apoptosis was determined by staining cells with Annexin V-FITC and PI labeling, using flow cytometry. Early apoptosis was characterized by plasma membrane reorganization and was detected by positive staining for Annexin V-FITC while later stage apoptosis indicating DNA damage showed positive staining for both Annexin V and PI (Lee et al., 2007). Hela cells were treated with 20 μg/ml PPT-LDH and PPT for 48 h before FACS analysis, meanwhile cells without any addition was set as control. As shown in Fig. 6(A), Hela cells without any addition showed 1.98% early apoptosis and 3.39% later apoptosis. The treatment with PPT led to 11.06% early apoptosis and 19.89% later apoptosis (Fig. 6B). Remarkably, when the cells were treated with PPT-LDH, the early apoptosis increased to 20.51% and later apoptosis increased to 33.11% (Fig. 6C). PPT can inhibit the assembly of tubulin into microtubules through interaction with protein at the colchicines binding site preventing the formation of the spindle consequently it induce the apoptotic processes (Roberts et al., 2008). The percentage of early apoptosis and later apoptosis in the PPT-LDH group both significantly increased compared with PPT alone and untreated control, which confirmed that PPT-LDH nanoparticles were able to induce the tumor cells apoptosis processes and readily led the cells to die. Therefore, PPT-LDH nanoparticles could be more taken up by Hela cells and LDH could protect PPT from rapid decomposition (Choy et al., 2004). The result also proved that PPT entrapped in LDH could enhance the efficient anti-tumor effect and LDH could serve as an excellent carrier system for anti-tumor drug.

3.5. In vivo anti-tumor effects of PPT-LDH nanoparticles

In vivo anti-tumor efficacy was evaluated by the treating nude mice bearing Hela tumor. As shown in Fig. 7, the results showed that the tumor growth exhibited a significant difference compared with saline control group ($p < 0.01$), indicating the reliable data and reasonable error. The remarkable therapeutic effect of PPT-LDH was demonstrated by the statistical significance of tumor weight and volume between mice injected with PPT-LDH and saline ($p < 0.01$). However, the free PPT, when administered at the molar equivalent dose, was not more effective as PPT-LDH, which revealed a higher anti-tumor effect of PPT-LDH in vivo. Tumor inhibition rates were calculated and are shown in Table 1. In the same way, mice injected with PPT-LDH had 46.39% inhibition rate, which was higher than that treated with free PPT.

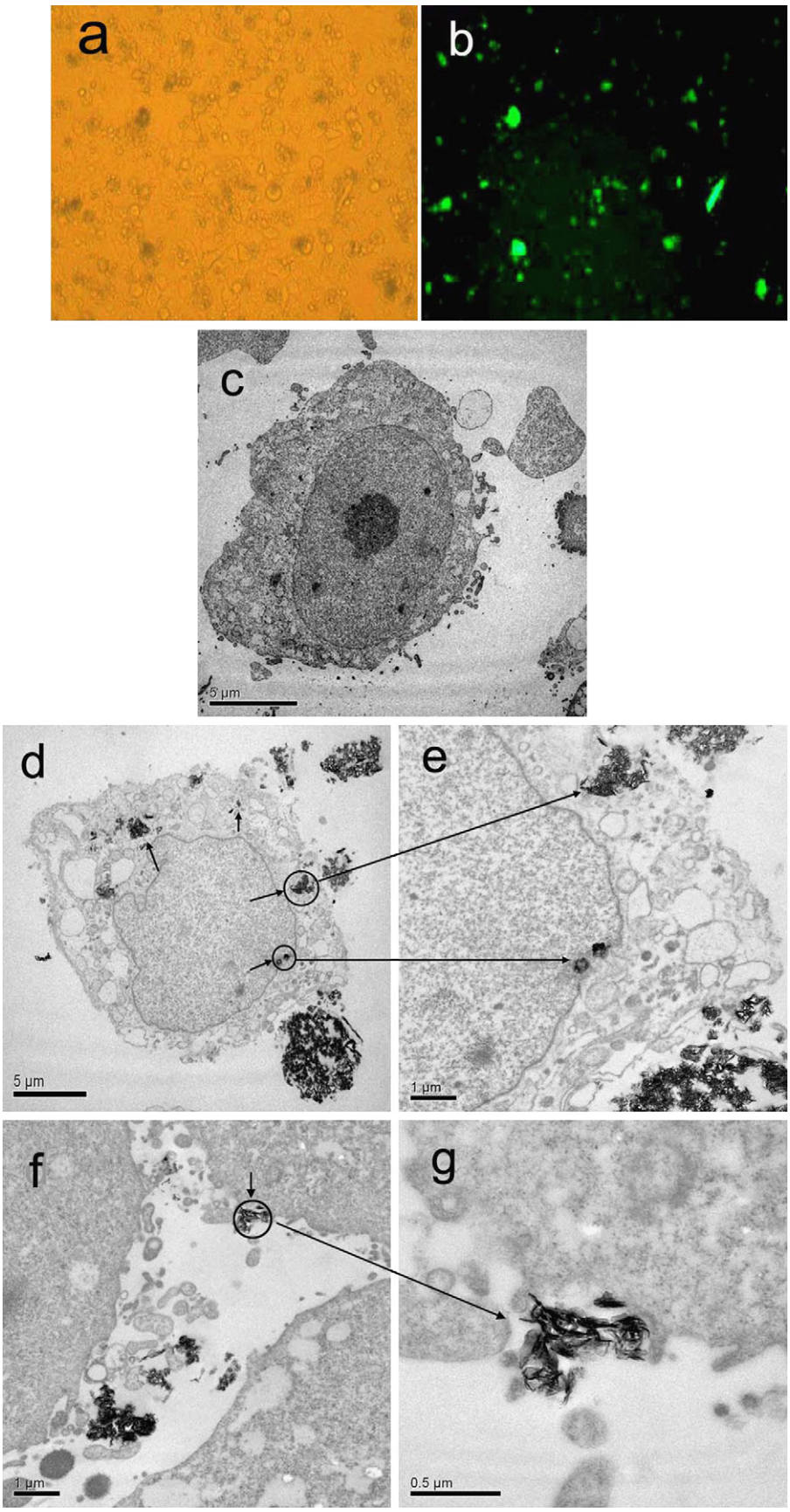

Fig. 4. Fluorescence image after Hela cells treated with PPT-LDH, cells exposed to PPT-LDH under white light (A) and PPT-LDH under blue light (B). Ultrastructure of Hela cells treated with PPT-LDH analyzed by TEM. Nanoparticles (arrow) were observed in Hela cells after incubation for 48 h: Hela + PBS (C), Hela + PPT-LDH (D–G).

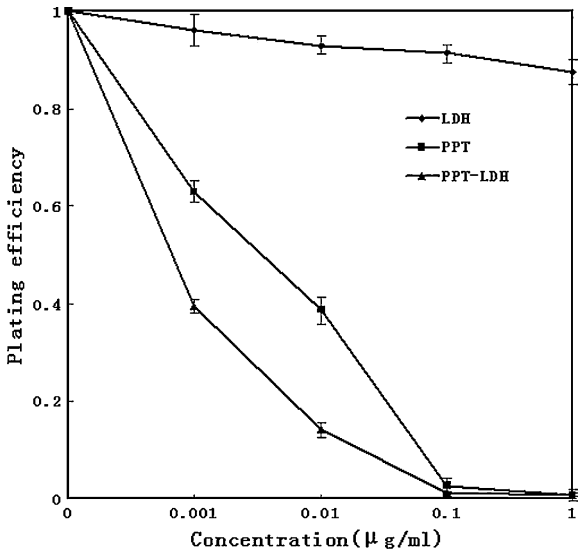

Fig. 5. Long-term proliferation of Hela cells after 14 days treatment with LDH, PPT and PPT-LDH at various concentrations in the colony forming efficiency assay. Values are represented as ratios of treated over corresponding control and represent mean ± SEM of at least three independent experiments.

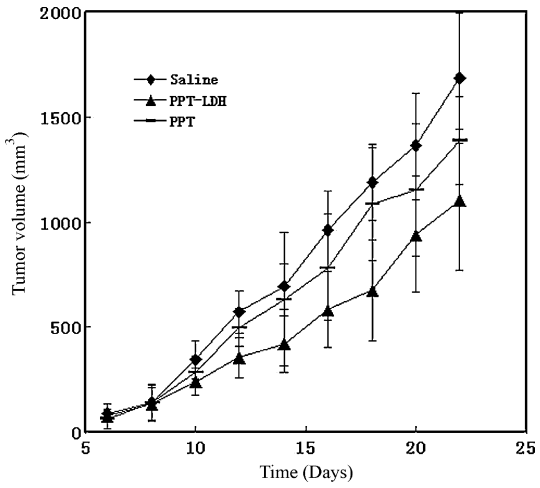

Fig. 7. In vivo anti-tumor effect by i.p. injection of PPT and LDH-PPT at a dose of 5 mg PPT/kg in nude mice bearing Hell cells evaluated by solid tumor growth.

In addition, the mice body weights were monitored throughout the test period as an indication of adverse effects of the drug. Table 1 shows the inhibition of weight gain in mice injected with PPT. In our preliminary experiment, furthermore, high doses of PPT were found to have a life-threatening toxicity to mice (data not shown). On the contrary, PPT loaded in LDH showed a much lower toxicity, as shown by the continues body weight gain of mice administered with PPT-LDH, which represents a reduced side effect of PPT. Thus, compared with free PPT, PPT-LDH was demonstrated to be more curative and less toxic to the mice.

3.6. Pharmacokinetics properties of PPT-LDH nanoparticles

The pharmacokinetic behavior of PPT incorporated in LDH was assessed in nude mice after intraperitoneal administration. Plasma clearance profiles of PPT-LDH were compared with that of free PPT at the molar equivalent dose. Serum PPT concentration was measured by HPLC. The results showed that both the two groups exhibited two-compartment model, which had an initial redistribution phase with a short half-life ($t_{1/2}\alpha$) followed by an elimination phase with a longer half-life ($t_{1/2}\beta$). As shown in Fig. 8, PPT had quick redistribution and clearance but PPT-LDH displayed a longer systemic circulation time suggesting its greater in vivo stability.

Pharmacokinetic parameters are listed in Table 2. Encapsulation of PPT in LDH obtained marked differences in terms of the pharmacokinetic parameters. Using LDH as carriers, a threefold enhancement of *AUC* was acquired, with a threefold reduction of *CL*, which suggested the increase of PPT entering body, and the decrease of PPT eliminated by organism, respectively. Furthermore, animals administered with PPT-LDH exhibited a delayed time to peak concentration compared with those treated with free PPT. Moreover, PPT-LDH distribution half-life ($t_{1/2}\alpha$) and elimination half-life ($t_{1/2}\beta$) were all about two times than PPT alone. Con-

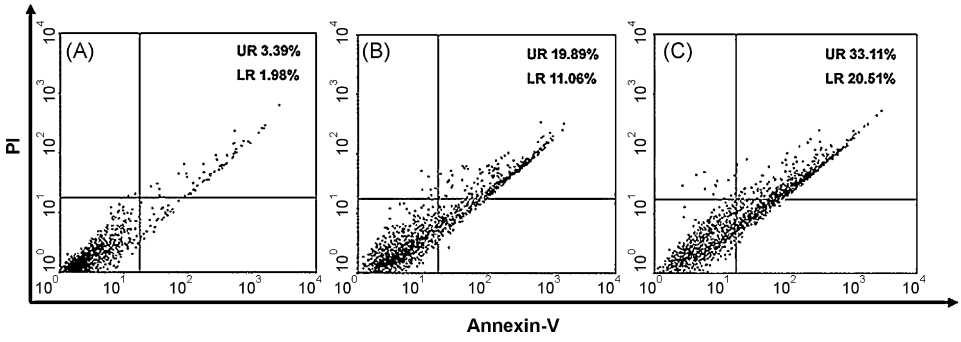

Fig. 6. FACS analysis of Hela cells stained with Annexin V-FITC and PI. (A) Cells did not treat with any agents for blank control. (B) Cells apoptosis induced by PPT. (C) Cells treated with the PPT-LDH. In all panels, LR represents early apoptosis and UR represents late apoptosis.

Table 1
Anti-tumor effect of different drug formulation reflected by body weight, tumor mass, and tumor inhibition rate.

Drug formulation	Body weight at different times (g)		Tumor mass (g)	Tumor inhibition rate (%)
	Initial drug delivery	Last drug delivery		
Saline	19.53 ± 1.82	31.82 ± 2.86	1.89 ± 0.42	
PPT-LDH	19.64 ± 1.47	30.79 ± 3.07	1.01 ± 0.15**	46.39
PPT	20.11 ± 1.93	18.25 ± 2.41	1.18 ± 0.28*	37.63

* Statistical significance is $p < 0.05$.
** Statistical significance is $p < 0.01$.

Table 2
Pharmacokinetic parameters (mean ± S.D.) of PPT after i.p. administration of PPT and PPT-LDH to mice with dose of 10 mg/kg in PPT.

	AUC (μg ml^{-1} h)	CL (mg/kg/h/μg ml^{-1})	T_{max} (h)	C_{max} (μg ml^{-1})	$t_{1/2}\alpha$ (h)	$t_{1/2}\beta$ (h)
PPT	34.32 ± 4.56	0.29 ± 0.02	1.44 ± 0.08	4.13 ± 0.37	0.91 ± 0.08	9.82 ± 8.50
PPT-LDH	109.66 ± 32.51	0.09 ± 0.002	2.19 ± 0.35	4.24 ± 2.13	1.78 ± 0.61	22.57 ± 3.95

AUC: area under serum concentration–time curve; *CL*: total body clearance; C_{max}: maximum serum concentration; T_{max}: time to reach C_{max}; $t_{1/2}\alpha$: distribution half-life; $t_{1/2}\beta$: elimination half-life.

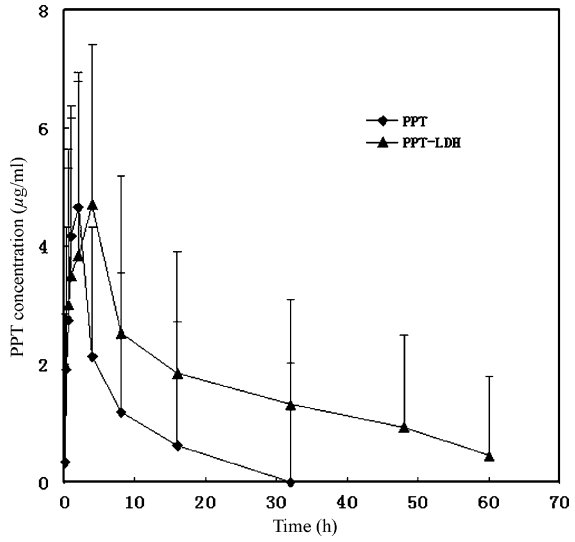

Fig. 8. Plasma concentration vs. time curves for PPT and PPT-LDH in mice. PPT and PPT-LDH formulations were administered via i.p. injection at a dose of 10 mg/kg in PPT. Each data point was the average of three to five animals and error bar equaled one standard deviation.

ceivably, the sustained release and slow clearance of PPT-LDH nanoparticles were favorable to the suppression of tumor and may account for the in vivo efficacy experiment. Overall, there is the potential for a broad range of new therapeutic applications using LDH as drug carrier.

4. Conclusions

Drug–inorganic nanohybrids were obtained by the hybridization of PPT with the LDH by intercalation method. The restrain ratio to tumor cells was enhanced by PPT-LDH which was also examined to have an effective long-term anti-tumor effect and increase the tumor cells apoptotic processes in vitro. In addition, PPT-LDH nanoparticles via intraperitoneal administration significantly decreased tumor growth and showed low toxicity in vivo. Pharmacokinetics study displayed a prolonged circulation time, and an increased bioavailability of PPT-LDH than that of PPT. Therefore, LDH can be considered as one of the ideal carriers for anti-tumor drugs and drug-LDH can be widely applied in the future anti-tumor chemotherapy.

Acknowledgements

The work was financially supported by the National Natural Science Foundation of China (No. 50673078), The National Basic Research Program of China (973 Program) (No. 2010CB912604), The 863 project of the Ministry of Science and Technology (No. 2007AA022004 and 2007AA021802), Shanghai Educational Development Foundation (Grant no. 2008CG26), Program for Young Excellent Talents in Tongji University (2007KJ062) and Shanghai key laboratory of cell signaling and diseases (No. 09DZ2260100).

References

Aisawa, S., Takahashi, S., Ogasawara, W., Umetsu, Y., Narita, E., 2001. Direct intercalation of amino acids into layered double hydroxides by coprecipitation. J. Solid State Chem. 162, 52–62.
Ambrogi, V., Famiani, F., Perioli, L., Marmottini, F., Di Cunzolo, I., Rossi, C., 2006. Effect of MCM-41 on the dissolution rate of the poorly soluble plant growth regulator, the indole-3-butyric acid. Micropor. Mesopor. Mater. 96, 177–183.
Ambrogi, V., Grandolini, G., Perioli, L., Giusti, L., Lucacchini, A., Martini, C., 1995. Studies on annulated 1,4-benzothiazines and 1,5-benzothiazepines. IX. Imidazo [2,1-d][1,5] benzothiazepines: synthesis and in vitro benzodiazepine receptor affinity. Eur. J. Med. Chem. 30, 429–437.
Arnold, A.M., 1979. Podophyllotoxin derivative VP 16-213. Cancer Chemother. Pharmacol. 3, 71–80.
Azzam, T., Domb, A.J., 2004. Current development in gene transfection agents. Curr. Drug Deliv. 1, 165–193.
Canel, C., Moraes, R.M., Dayan, F.E., Ferreira, D., 2000. Podophyllotoxin. Phytochemistry 54, 115–120.
Choy, J.H., Jung, J.S., Oh, J.M., Park, M., 2004. Layered double hydroxides as an efficient drug reservoir for folate derivatives. Biomaterials 25, 3059–3064.
Choy, J.H., Kim, Y.I., Kim, B.W., Campet, G., Portier, J., Huong, P.V., 1999. Grafting mechanism of electrochromic PAA–WO_3 composite film. J. Solid State Chem. 142, 368–373.
Choy, J.H., Yoon, J.B., Park, J.H., 2001. In situ XAFS study at the Zr K-edge for SiO_2/ZrO_2 nano-sol. J. Synchrotron Radiat. 8, 782–784.
Del Arco, M., Gutierrez, S., Martin, C., Rives, V., Rocha, J., 2000. Effect of the Mg:Al ratio on borate (or silicate)/nitrate exchange in hydrotalcite. J. Solid State Chem. 151, 272–280.
Garnett, M.C., 2004. Gene-delivery systems using cationic polymers. Crit. Rev. Ther. Drug Carrier Syst. 16, 147–207.
Gordaliza, M., Castro, M.A., Del Corral, J.M., Feliciano, A.S., 2000. Antitumor properties of podophyllotoxin and related compounds. Curr. Pharm. Des. 6, 1811–1839.
Greenspan, E.M., Leiter, J., Shear, M.J., 1950. Effect of alpha-peltatin, beta-peltatin, podophyllotoxin on lymphomas and other transplanted tumors. J. Natl. Cancer Inst. 10, 1295–1333.
Gutierrez, S., Carbonell, E., Galofrea, P., Xamena, N., Creus, A., Marcos, R., 1995. A cytogenetic follow-up study of thyroid cancer patients treated with 131I. Cancer Lett. 91, 199–204.
Hainswoth, J.D., Williams, S.D., Einhorn, L.H., Birch, R., Greco, F.A., 1985. Successful treatment of resistant germinal neoplasms with VP-16 and cisplatin: results of a Southeastern cancer study group trial. J. Clin. Oncol. 3, 666–671.
Hibino, T., Nishiyama, T., 2004. Role of TGF-β2 in the human hair cycle. J. Dermatol. Sci. 35, 9–18.
Hofer, C., Teichert, C., Wachter, M., Bobek, T., Lyutovich, K., Kasper, E., 2004. Nanostructure formation on ion-eroded SiGe film surfaces. Superlatt. Microstruct. 36, 281–291.
Imbert, T.F., 1998. Discovery of podophyllotoxins. Biochimie 80, 207–222.
Kwak, S.Y., Kriven, W.M., Wallig, M.A., Choy, J.H., 2004. Inorganic delivery vector for intravenous injection. Biomaterials 25, 5995–6001.
Kwon, S.J., Choy, J.H., 2003. A novel hybrid of Bi-based high-Tc superconductor and molecular complex. Inorg. Chem. 42, 8134–8136.
Lee, M.K., Lim, S.J., Kim, C.K., 2007. Preparation, characterization and in vitro cytotoxicity of paclitaxel-loaded sterically stabilized solid lipid nanoparticles. Biomaterials 28, 2137–2146.
Li, B., He, J., Evans, D.G., Duan, X., 2004. Enteric-coated layered double hydroxides as a controlled release drug delivery system. Int. J. Pharm. 287, 89–95.
Longstaff, E., Von Krogh, G., 2001. Condyloma eradication: self-therapy with 0.15–0.5% podophyllotoxin versus 20–25% podophyllin preparations—an integrated safety assessment. Regul. Toxicol. Pharmacol. 33, 117–137.
Nakayama, H., Hayashi, A., Eguchi, T., Nakamura, N., Tsuhako, M., 2002. Adsorption of formaldehyde by polyamine-intercalated α-zirconium phosphate. Solid State Sci. 4, 1067–1070.
Qin, L.L., Wang, S.L., Zhang, R., Zhu, R.R., Sun, X.Y., Yao, S.D., 2008. Two different approaches to synthesizing Mg–Al–layered double hydroxides as folic acid carriers. J. Phys. Chem. Solids 69, 2779–2784.
Roberts, J.E., Wielgus, A.R., Boyes, W.K., Andley, U., Chignell, C.F., 2008. Phototoxicity and cytotoxicity of fullerol in human lens epithelial cell. Toxicol. Appl. Pharmacol. 228, 49–58.
Seida, Y., Nakano, Y., 2002. Removal of phosphate by layered double hydroxides containing iron. Water Res. 36, 1306–1312.
Shah, J.C., Chen, J.R., Chow, D., 1989. Preformulation study of etoposide: identification of physicochemical characteristics responsible for the low and erratic oral bioavailability of etoposide. Pharm. Res. 6, 408–412.

Taylor, R.M., 1984. The rapid formation of crystalline double hydroxyl salts and other compounds by controlled hydrolysis. Clay Miner. 19, 591–603.
Tyner, K.M., Schiffman, S.R., Giannelis, E.P., 2004. Nanobiohybrids as delivery vehicles for camptothecin. J. Control. Rel. 95, 501–514.
Van-maanen, J.M.S., Retal, J., De-vries, J., Pincedo, H.M., 1998. Mechanism of action of antitumor drug etoposide: a review. J. Natl. Cancer Inst. 80, 1526–1533.
Wang, G., Feng, L., Luck, R.L., Evans, D.G., Wang, Z., Duan, X., 2005. Sol–gel synthesis, characterization and catalytic property of silicas modified with oxomolybdenum complexes. J. Mol. Catal. A: Chem. 241, 8–14.
Wong, K.W., Colfen, H., Whilton, N.T., Douglas, T., Mann, S., 1999. Synthesis and characterization of hydrophobic ferritin proteins. J. Inorg. Biochem. 76, 187–195.
Xu, Z.P., Zeng, Q.H., Lu, G.Q., Yu, A.B., 2006. Inorganic nanoparticles as carriers for efficient cellular delivery. Chem. Eng. Sci. 61, 1027–1040.
Xu, Z.P., Niebert, M., Porazik, K., Walker, T.L., Cooper, H.M., 2008. Subcellular compartment targeting of layered double hydroxide nanoparticles. J. Control. Rel. 130, 86–94.
Xue, Y.H., Zhang, R., Sun, X.Y., Wang, S.L., 2007. The construction and characterization of layered double hydroxides as delivery vehicles for podophyllotoxins. Mater. Sci. Mater. Med. 8, 1197–1202.
Yuan, H., Miao, J., Du, Y.Z., You, J., 2008. Cellular uptake of solid lipid nanoparticles and cytotoxicity of encapsulated paclitaxel in A549 cancer cell. Int. J. Pharm. 348, 137–145.
Zhang, H., Qi, R., Evans, D.G., Duan, X., 2004. Synthesis and characterization of a novel nano-scale magnetic solid base catalyst involving a layered double hydroxide supported on a ferrite core. J. Solid State Chem. 177, 772–780.
Zhang, H., Zou, K., Guo, S., Duan, X., 2006. Nanostructural drug–inorganic clay composites: structure, thermal property and in vitro release of captopril-intercalated Mg–Al–layered double hydroxides. J. Solid State Chem. 179, 1792–1801.
Zhang, H., Zou, K., Sun, H., Duan, X., 2005. A magnetic organic–inorganic composite: synthesis and characterization of magnetic 5-aminosalicylic acid intercalated layered double hydroxides. J. Solid State Chem. 178, 3485–3493.